Large absolute photonic band gaps created by rotating noncircular rods in two-dimensional lattices

Xue-Hua Wang*
Institute of Physics, Academia Sinica, P.O. Box 603, Beijing 100080, China

Ben-Yuan Gu, Zhi-Yuan Li, and Guo-Zhen Yang
CCAST (World Laboratory), P.O. Box 8730, Beijing 100080, China
and Institute of Physics, Academia Sinica, P.O. Box 603, Beijing 100080, China
(Received 18 June 1999)

Absolute photonic band gaps (PBG's) can be substantially improved in two-dimensional (2D) lattices by rotating noncircular air rods in dielectric background, in which the configuration of high-dielectric regions that are both practically isolated and linked by narrow veins can be freely adjusted to create large absolute PBG's. For square lattice, the largest absolute PBG's in the single-square-rod and double-hybrid-rods structures are 315 and 150 % sizes of those in the corresponding single-circular-rod and double-circular-rods structures, respectively. Furthermore, the large absolute PBG's persist in a wide range of filling fractions and reach their maxima far away from the close-packed conditions, and this is in vast favor of preparation of crystals. Such an approach is also applicable to other 2D lattices. It may open up a scope for engineering PBG's.
[S0163-1829(99)10639-8]

Since the pioneering work of Yablonovitch and John,[1,2] there appears to be great interest in fabricating the photonic band-gap (PBG) structures in recent years. These structures exhibit ''forbidden'' frequency region where electromagnetic waves cannot propagate along any direction. This may bring about some peculiar physical phenomena,[3–5] as well as wide applications in several scientific and technical areas.[6,7] Although three–dimensional (3D) PBG structures will provide the most stirring potential in applications and the preparation of 3D crystals in the visible or infrared regime has very recently been reported,[8,9] fabricating 3D crystals with the available PBG's is still an overwhelming challenge. In contrast, two-dimensional (2D) crystals with the available PBG's in this regime have been successfully fabricated.[10–13] Furthermore, 2D PBG structures could also find some important uses such as a feedback mirror in laser diodes.[14] Perhaps for this reason, much attention has been drawn towards 2D PBG structures.

One of the most severe limits to the formation of absolute PBG's comes from degeneracy of photonic bands at high-symmetry points in the Brillouin zone. Many approaches have been proposed to lift this limit and then to produce the absolute PBG's as large as possible. Very recently, it is reported that a dielectric anisotropy sufficient enough in the scattering elements can break the degeneracy of photonic bands and then produce partial band gaps for 3D photonic crystals,[15] and this anisotropy can also lead to a large absolute PBG in 2D lattices.[16] Before this, it was shown that the absolute PBG's can be increased by introducing a two-point basis set in 2D lattices,[17] quite similar to the 3D diamond structures.[18] In earlier studies, the noncircular rods were utilized to lift the band degeneracy in 2D lattices.[19] But, this attempt failed to both open the absolute PBG for the refractive index contrast less than 3.51 and create a larger absolute PBG than that by conventional circular rods. Perhaps for this reason, rare attention has been paid to 2D arrays of noncircular rods thereafter. However, in this paper we will demonstrate that the approach of rotating noncircular rods in 2D lattices here presented is very powerful in opening and improving the absolute PBG's.

It is well known that there exists for 2D photonic crystals the general rule of thumb:[7] The absolute PBG's are favored in compromise crystals with high-dielectric regions that are both practically isolated and linked by narrow veins. It is difficult to fabricate this sort of crystals with too thin veins. Thus, it is natural to choose in priority the one with a filling faction f far less than the close–packed one from different crystals possessing absolute PBG's of equal size. 2D lattices of noncircular air rods in a dielectric background may be the promising candidates as the above crystals as the shape and orientation of narrow–veins can be freely adjusted by rotating the noncircular rods and then fruitful configuration of high-dielectric regions can be formed. Our numerical simulations will show that a large absolute PBG is really present in those crystals over rather a wide range of filling fractions and reaches its maximum size far away from the close–packed conditions.

For simplicity and not without generality, we prefer to focus on the 2D square lattices of the air rods in a dielectric background. The schematic diagram of crystals is shown in Fig. 1: (a) single-square-rod structures in which square rods lie at corners of unit cells; (b) double-hybrid-rods structures in which circular rods are added into centers of unit cells. The corresponding structures in which square rods are replaced by circular rods are referred to as the single-circular-rod and double-circular-rods structures, respectively. θ in Fig. 1(a) represents the angle between axes of the square cross section and the 2D lattices.

The photonic band structures of the above crystals can be obtained by solving Maxwell's equations with use of plane–wave expansion method.[15,18,20–22] Maxiwell's equations are combined to give the wave equation in terms of the magnetic field **H**

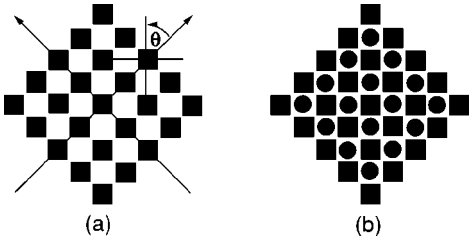

FIG. 1. Schematic diagrams of 2D square lattices of air rods in a dielectric background: (a) single-square-rod structures; (b) double-hybrid-rods structures.

$$\nabla\times[\epsilon^{-1}(\mathbf{r})\nabla\times\mathbf{H}]=\frac{\omega^2}{c^2}\mathbf{H}, \tag{1}$$

where $\epsilon(\mathbf{r})$ is position−dependent dielectric constant, $\mathbf{r}=(x,y)$ lies in the plane normal to the rods, ω is the frequency, and c is the speed of light in vacuum. The magnetic field $\mathbf{H}(\mathbf{r})$ and the dielectric function $\epsilon(\mathbf{r})$ can be expanded in a series of plane waves

$$\mathbf{H}(\mathbf{r})=\sum_{\mathbf{G}}\sum_{j=1,2}H_{\mathbf{G},j}\hat{\mathbf{e}}_j e^{i(\mathbf{k}+\mathbf{G})\cdot\mathbf{r}}, \tag{2}$$

$$\epsilon(\mathbf{r})=\sum_{\mathbf{G}}\epsilon(\mathbf{G})e^{i\mathbf{G}\cdot\mathbf{r}}, \tag{3}$$

where $\mathbf{k}$ is the wave vector in the first Brillouin zone and $\mathbf{G}=(G_x,G_y)$ is a reciprocal-lattice vector. The unit vectors $\hat{\mathbf{e}}_j$ are orthogonal to $(\mathbf{k}+\mathbf{G})$ and the coefficients $H_{\mathbf{G},j}$ are the corresponding components of the magnetic field. The Fourier coefficients $\epsilon(\mathbf{G})$ are defined as

$$\epsilon(\mathbf{G})=\frac{1}{S}\int_S\epsilon(\mathbf{r})e^{-i\mathbf{G}\cdot\mathbf{r}}d\mathbf{r}, \tag{4}$$

where the integration is carried out over the area S of one lattice unit cell. The analysis of Eq. (1) can be reduced to solving two standard eigenvalue equations, each describing a particular wave polarization. They are given as follows:

$$\sum_{\mathbf{G}'}|\mathbf{k}+\mathbf{G}||\mathbf{k}+\mathbf{G}'|\epsilon^{-1}(\mathbf{G}-\mathbf{G}')H_{\mathbf{G}',1}=\frac{\omega^2}{c^2}H_{\mathbf{G},1}, \tag{5}$$

for E−polarization mode with the electric field vector parallel to the rod axes and

$$\sum_{\mathbf{G}'}(\mathbf{k}+\mathbf{G})(\mathbf{k}+\mathbf{G}')\epsilon^{-1}(\mathbf{G}-\mathbf{G}')H_{\mathbf{G}',2}=\frac{\omega^2}{c^2}H_{\mathbf{G},2}, \tag{6}$$

for H−polarization mode with magnetic field vector parallel to the rod axes. Here, $\epsilon^{-1}(\mathbf{G}-\mathbf{G}')$ is the inverse of the matrix $\epsilon(\mathbf{G}-\mathbf{G}')$ with the elements defined by Eq. (4). All structural information of the crystals is contained in the coefficient matrix $\epsilon(\mathbf{G}-\mathbf{G}')$. The integral in Eq. (4) can be expanded and simplified to give

$$\epsilon(\mathbf{G})=\begin{cases}\epsilon_b+f(\epsilon_a-\epsilon_b) & \mathbf{G}=0,\\ (\epsilon_a-\epsilon_b)I(\mathbf{G}) & \mathbf{G}\neq 0,\end{cases} \tag{7}$$

where ϵ_a and ϵ_b are the dielectric constants of the rods and background, respectively; $f=S_d/S$ is the rod filling fraction (S_d the cross−section area of the rods in a lattice unit cell); the geometric factor $I(\mathbf{G})$ is defined as

$$I(\mathbf{G})=\frac{1}{S}\int_{S_d}e^{-i\mathbf{G}\cdot\mathbf{r}}d\mathbf{r}. \tag{8}$$

Here, the integral is now over the rods in a lattice unit cell. We introduce $I_{ss}(\mathbf{G})$, $I_{sc}(\mathbf{G})$, $I_{dh}(\mathbf{G})$, and $I_{dc}(\mathbf{G})$ to denote the geometric factors of the single-square-rod, single-circular-rod, double-hybrid-rods, and double-circular-rods structures, respectively. They can be easily expressed as

$$I_{ss}(\mathbf{G})=\frac{1}{S}F(\tilde{G}_x,C)F(\tilde{G}_y,C), \tag{9}$$

$$I_{sc}(\mathbf{G})=\frac{1}{S}2\pi G^{-1}R_0J_1(GR_0), \tag{10}$$

$$I_{dh}(\mathbf{G})=I_{ss}(\mathbf{G})+I_{sc}(\mathbf{G})\cos\alpha, \tag{11}$$

$$I_{dc}(\mathbf{G})=I_{sc}(\mathbf{G})(1+\cos\alpha), \tag{12}$$

where C is the side length of the square cross section; R_0 the radius of the circular cross section; $\alpha=(G_x+G_y)a/2$, a is the lattice constant; $G=|\mathbf{G}|$; J_1 is the first-order Bessel function of the first kind. In Eq. (9), $F(K,X)$ and $\tilde{\mathbf{G}}$ are defined as

$$F(K,X)=\begin{cases}X & K=0,\\ 2K^{-1}\sin(KX/2) & K\neq 0,\end{cases} \tag{13}$$

$$\begin{pmatrix}\tilde{G}_x\\ \tilde{G}_y\end{pmatrix}=\begin{pmatrix}\cos\theta & \sin\theta\\ -\sin\theta & \cos\theta\end{pmatrix}\begin{pmatrix}G_x\\ G_y\end{pmatrix}, \tag{14}$$

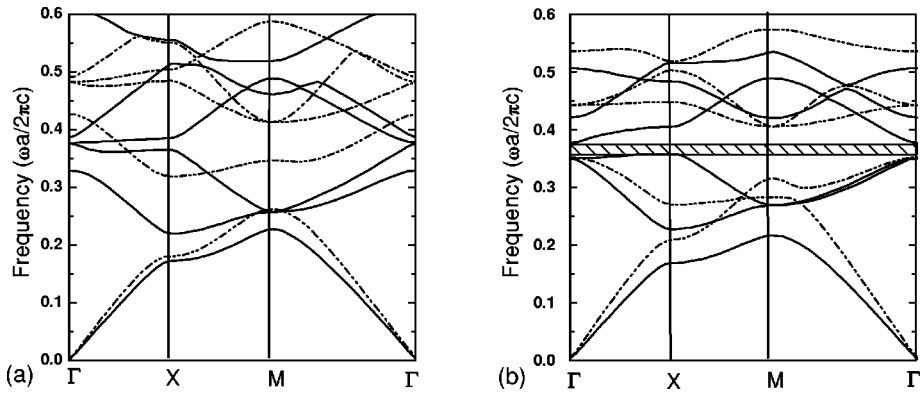

FIG. 2. Photonic band structures of the single-square-rod structures with $n_b=3.4$ at $f=0.5$: (a) $\theta=0°$, and (b) $\theta=45°$. The solid and dash-dot-dotted lines correspond to the E- and H-polarization modes, respectively.

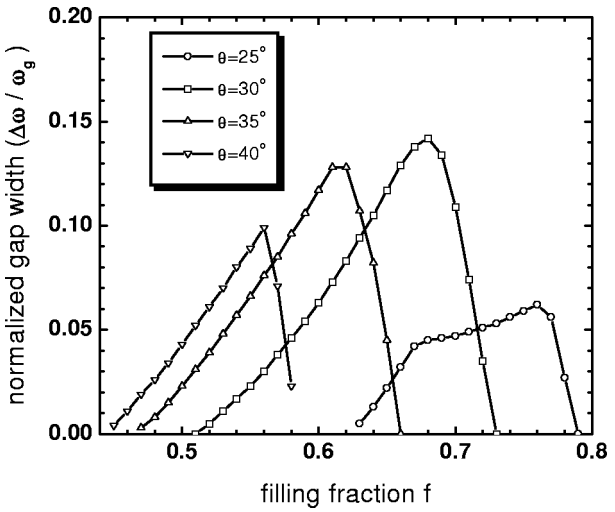

FIG. 3. Dependence of the normalized gap width of the absolute PBG on the filling fraction f in the single-square-rod structures with $n_b=3.4$ for four different rotation angles of $\theta=25°$, 30°, 35°, 40°.

where θ is the rotational angle of the square rods.

The results that follow were obtained from Eqs. (5) and (6) using 625 plane waves and the convergence accuracy for the lowest ten photonic bands is better than 1%.

We first consider the single-square-rod structures in which the refractive index of dielectric background is $n_b=3.4$. The photonic band structures are displayed in Figs. 2(a) for $\theta=0°$ and 2(b) for $\theta=45°$ at the filling fraction of $f=0.5$, respectively. The absolute PBG is not present at $\theta=0°$, as seen in Fig. 2(a). More detailed numerical calculations also show that there is no absolute PBG for any filling fraction at this orientation. These results show that breaking the circular symmetry of rods is not sufficient to open the absolute PBG for the refractive index of 3.4. This can be changed by rotating the square rods, as shown in Fig. 2(b). Overlapping of nontouching H 2–3 bands is removed, and degeneracy of E 3–4 bands at Γ point is lifted. This opens E 3–4 and H 2–3 band gaps, which overlap with each other and create an absolute band gap with a magnitude of $\Delta\omega=0.02(2\pi c/a)$ and a normalized width of $\Delta\omega/\omega_g=5.4\%$. Here, ω_g is the midgap frequency. Although the absolute PBG is not large, it has verified that adjusting the orientation of the noncircular crosssection can be utilized to engineer PBG's.

Note that the close–packed filling fraction of the single-square-rod structure with $\theta=45°$ is $f_{cp}=0.5$, which may limit the size of the absolute PBG. It should be expected that there exist larger absolute PBG's for some rotation angles with f_{cp} larger than 50%. The normalized widths of the absolute PBG's as functions of the filling fraction are displayed in Fig. 3 for $\theta=25°$, 30°, 35°, and 40°, corresponding to $f_{cp}=0.821$, 0.75, 0.671, and 0.587, in turn. Three crystals except for $\theta=25°$ can create larger absolute PBG's. Among them, the one with $\theta=30°$ possesses the largest absolute PBG of $\Delta\omega=0.063(2\pi c/a)$ and $\Delta\omega/\omega_g=14.2\%$ at $f=0.68$, quite away from $f_{cp}=0.75$. In this crystal, the smallest width of the narrow veins is $0.0478a$, not too thin for modern lithography. Furthermore, the $\Delta\omega/\omega_g$ exceeds 10% at the range of $0.63\leqslant f\leqslant 0.70$ and vanishes near the closed–packed structure. In contrast, the largest absolute PBG in the corresponding single-circular-rod crystal is reached at $f=0.78$, very close to $f_{cp}=0.785$. Here, its magnitude and normalized width become $\Delta\omega=0.02(2\pi c/a)$ and $\Delta\omega/\omega_g=4\%$, 215 and 255% smaller than those in the single-square-rod structure with $\theta=30°$.

We now examine the double-hybrid-rods structures, in which more fruitful patterns of the high-dielectric regions and narrow veins can be formed by rotating the square rods and this will help to create larger absolute PBG's. For these structures, we define a parameter β as the ratio of the diameter of circular rods to the side length of square rods. In the following calculations, the refractive index is taken as $n_b=3.6$. The photonic band structures for $f=0.65$ and $\beta=0.64$ are plotted in Fig. 4(a) at $\theta=0°$ and Fig. 4(b) at $\theta=26°$. It can be seen that there is no any absolute PBG for $\theta=0°$. However, rotating the square rods can remove overlapping of nontouching H 2−3 bands and lift degeneracy of E 4−5 bands rather than that of E 3−4 bands in the single-square-rod structures. H 2−3 and E 4−5 band gaps overlap with each other and create a large absolute PBG with $\Delta\omega=0.068(2\pi c/a)$ and $\Delta\omega/\omega_g=14.5\%$ at $\theta=26°$. These results show that the absolute PBG's cannot be opened by both breaking circular symmetry of rods and introducing two–point basis set in the lattice if the noncircular rods are not rotated. Thus, rotation of noncircular rods plays a key role in opening the absolute PBG's. To get better insight into superior features of the double-hybrid-rods structures, we investigate in detail the dependence of PBG's on physical parameters as β, θ, and f.

Figure 5 displays the dependence of the positions of the H 2-3 and E 4-5 band gaps on the parameter β at $\theta=26°$ for $f=0.60$, 0.65, and 0.70. The optimum overlap of the H 2−3 and E 4−5 band gaps occurs at $\beta=0.64$, 0.63, 0.62, in

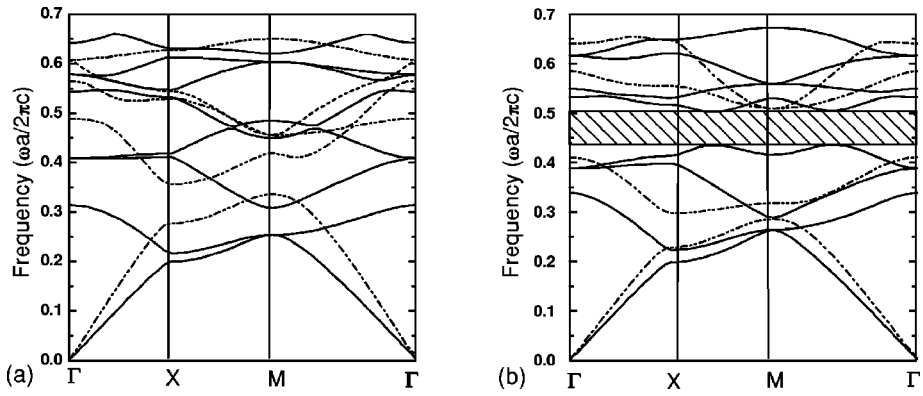

FIG. 4. Photonic band structures of the double-hybrid-rods structures with $n_b=3.6$ at $\beta=0.64$ and $f=0.65$: (a) for $\theta=0°$ and (b) for $\theta=26°$. The solid and dash-dot-dotted lines correspond to the E- and H-polarization modes, respectively.

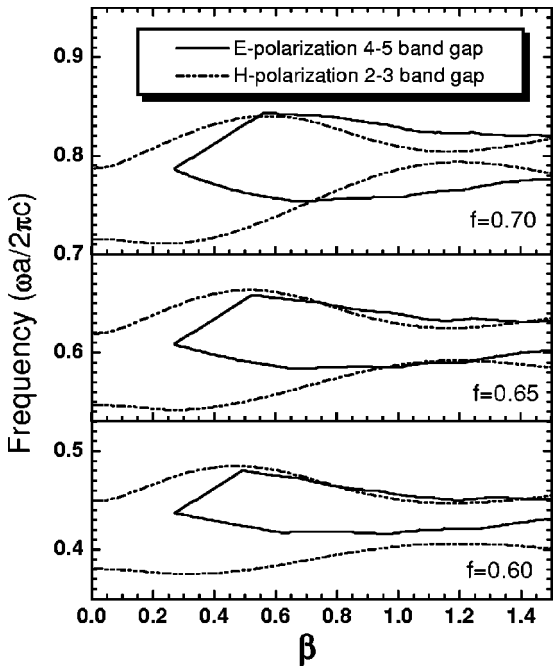

FIG. 5. Positions of the H 2−3 and E 4−5 band gaps as functions of the parameter β in the double-hybrid-rods structures with $n_b=3.6$ at $\theta=26°$ for three different filling fractions of $f=0.60$, 0.65, 0.70.

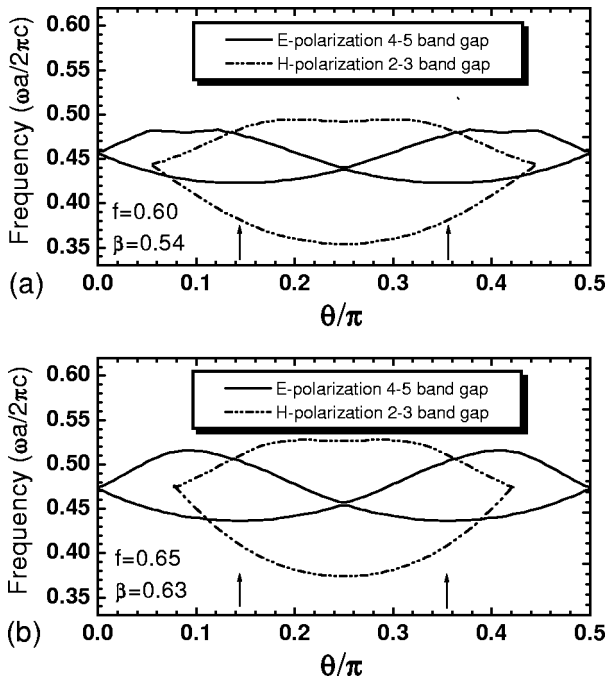

FIG. 6. Positions of the H 2−3 and E 4−5 band gaps as functions of the rotation angle θ/π in the double-hybrid-rods structures with $n_b=3.6$: (a) $f=0.60$, $\beta=0.54$, and (b) $f=0.65$, $\beta=0.63$.

turn, generating maximum absolute PBG's with $\Delta\omega_{max}=0.057$, 0.070, and $0.085(2\pi c/a)$, respectively. The large absolute PBG's can be persisted within a very wide range of parameter β, where we have $\Delta\omega_{max}-0.003(2\pi c/a)\leqslant\Delta\omega\leqslant\Delta\omega_{\max}$ for β values extending from 0.52 to 0.68 at $f=0.60$, 0.52 to 0.72 at $f=0.65$, and 0.56 to 0.70 at $f=0.7$. This is very beneficial to fabrication of photonic crystals.

In order to find the optimum rotation angle θ, we display the positions of the H 2-3 and E 4-5 band gaps as a function of θ in Fig. 6(a) for $f=0.6$ and $\beta=0.54$, and Fig. 6(b) for $f=0.65$ and $\beta=0.63$. The band gaps of both polarization modes exhibit excellent symmetry with respect to $\theta=45°$, as expected. In fact, it origins from the inverse symmetry of the crystal. The optimum overlapping between H 2-3 and E 4-5 band gaps occurs at $\theta=26°$ for the two cases. This fact seems to indicate that the optimum rotation angle is independent of the filling fraction f and the parameter β. We also examine the variation of normalized width of the absolute PBG with the filling fraction at $\beta=0.62$ for three different rotation angles of $\theta=20°,26°,30°$. The results are displayed in Fig. 7. It can be seen that the absolute BPG at $\theta=26°$ is larger than at both $\theta=30°$ and 20° for f from 0.53 to 0.74. By combining of Figs. 6 and 7, it makes sure that $\theta=26°$ is the optimum rotation angle over rather wide ranges of f and β.

As a comparison, we have carried out detailed numerical calculations for the double-circular-rods structures with $n_b=3.6$. The results show that the largest absolute PBG with $\Delta\omega=0.06(2\pi c/a)$ and $\Delta\omega/\omega_g=12\%$ is reached at $\beta=0.14$ and $f=0.793$, very close to the close–packed structure of $f_{cp}=0.8$. In contrast, it has been shown in Fig. 7 that the maximum absolute gaps in the double-hybrid-rods structures are achieved at $f=0.71$ for $\theta=26°$ and at $f=0.75$ for $\theta=30°$, both far away from the close–packed conditions with $f_{cp}=0.887$ and $f_{cp}=0.926$, respectively. Here, they have the normalized widths of 17.0% and 17.1%, and the magnitudes of $0.085(2\pi c/a)$ and $0.090(2\pi c/a)$, in turn. The magnitudes of both remarkably increase by 41.7 and 50.0 %, respectively in comparison with the largest PBG in the double-circular-rods structures. More importantly, the large absolute PBG can persist over a very wide range of the filling fractions. For $\theta=26°$, its normalized width still exceeds 10% even for f as low as 0.55. For f from 0.55 to 0.71, the smallest width of the narrow veins of crystal ranges from $0.1421a$ to $0.0704a$, that is to say,

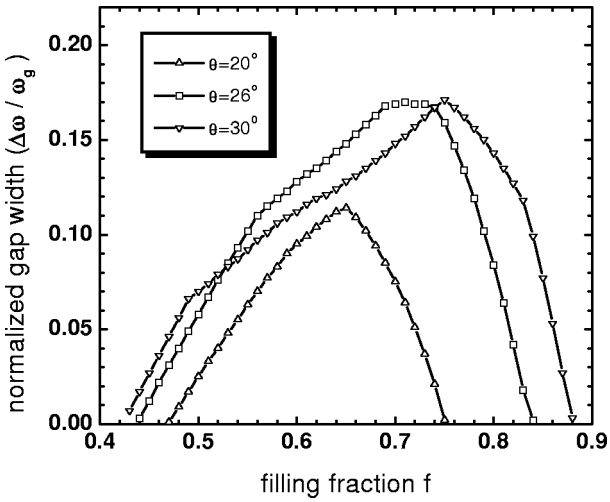

FIG. 7. Dependence of the normalized width of absolute PBG on filling fraction f in the double-hybrid-rods structures with $n_b=3.6$ at $\beta=0.62$ for three different rotation angles of $\theta=20°$, 26°, and 30°.

they are between $0.21315(\mu\mathrm{m})$ to $0.1056(\mu\mathrm{m})$ for a lattice constant of $a \approx 1.5(\mu\mathrm{m})$ in the near-infrared regime. This is very favorable to the fabrication of photonic crystals.

Finally, it is worth pointing out that the way of rotating the noncircular rods here presented is also applicable to other 2D lattices to create and improve absolute PBG's. Numerical calculations for 2D triangular lattice show that the single-hexagonal-rod structures with $n_b = 3.6$ can have a largest absolute PBG with $\Delta\omega = 0.105(2\pi c/a)$ and $\Delta\omega/\omega_g = 22.9\%$, also quite an advance over the corresponding single-circular-rod structures, here the largest absolute PBG is of $\Delta\omega = 0.092(2\pi c/a)$ and $\Delta\omega/\omega_g = 19.2\%$.

As a conclusion, we have investigated in detail the photonic band structures of 2D square lattices of noncircular air rods in dielectric background by plane–wave expansion method. Rotating the noncircular rods can freely adjust the configuration of high-dielectric regions that are both practically isolated and linked by narrow veins to both lift degeneracy of bands at high-symmetry points and remove overlapping of nontouching bands. Comparing with the previous methods, this method is more effective in opening absolute PBG's. Moreover, it can lead to both the remarkable improvements in sizes of the absolute PBG's and the substantial advancements in performance of the PBG structures. Numerical simulations show that the sizes of the largest absolute PBG's in the single-square-rods and double-hybrid-rods structures have remarkable increases of 215 and 50 % over those in the corresponding single-circular-rod and double-circular-rods structures, respectively. Furthermore, the large absolute PBG's can persist in rather a wide range of filling fractions and reach their maxima far away from the close–packed conditions, which are in vast favor of fabrication of photonic crystal by lithography. Such an approach is also applicable to other 2D lattices. It may open up a new scope for fabricating 2D photonic crystals with large absolute PBG's.

We gratefully acknowledge the financial support from the National Natural Science Foundation of China.

*Electronic address: wangxh@aphy.iphy.ac.cn

[1] E. Yablonovitch, Phys. Rev. Lett. **58**, 2059 (1987).
[2] S. John, Phys. Rev. Lett. **58**, 2486 (1987).
[3] S. John and J. Wang, Phys. Rev. B **43**, 12 772 (1991).
[4] S. John and T. Quang, Phys. Rev. A **50**, 1764 (1994).
[5] S. Y. Zhu, H. Chen, and H. Huang, Phys. Rev. Lett. **79**, 205 (1997).
[6] J. Opt. Soc. Am. B **10**, 208 (1993), special issue on development and applications of materials exhibiting photonic band gaps.
[7] J. D. Joannopouls, P. R. Villeneuve, and S. Fan, Nature (London) **386**, 143 (1997).
[8] J. E. G. J. Wijnhoven and W. L. Vos, Science **281**, 802 (1998).
[9] A. A. Zakhidov, R. H. Baughman, Z. Iqbal, C. X. Cui, I. Khayrullin, S. O. Dantas, J. Marti, and V. G. Ralchenko, Science **282**, 897 (1998).
[10] T. F. Krauss, R. De La Rue, and S. Band, Nature (London) **383**, 699 (1996).
[11] U. Grüning, V. Lehmann, S. Ottow, and K. Busch, Appl. Phys. Lett. **68**, 747 (1996).
[12] K. Inoue, M. Wada, K. Sakoda, M. Hayashi, T. Fukushima, and A. Yamanaka, Phys. Rev. B **53**, 1010 (1996).
[13] H.-B. Lin, R. J. Tonucci, and J. Campillo, Appl. Phys. Lett. **68**, 2927 (1996).
[14] D. L. Bullock, C. Shih, and R. S. Margulies, J. Cell. Sci. **10**, 399 (1993).
[15] Z. Y. Li, J. Wang, and B. Y. Gu, Phys. Rev. B **58**, 3721 (1998).
[16] Z. Y. Li, B. Y. Gu, and G. Z. Yang, Phys. Rev. Lett. **81**, 2574 (1998).
[17] C. M. Anderson and K. P. Giapis, Phys. Rev. Lett. **77**, 2949 (1996).
[18] K. M. Ho, C. T. Chan, and C. M. Soukoulis, Phys. Rev. Lett. **65**, 3152 (1990).
[19] P. R. Villeneuve and M. Piché, Phys. Rev. B **46**, 4969 (1992); **46**, 4973 (1992).
[20] K. M. Leung and Y. F. Liu, Phys. Rev. Lett. **65**, 2646 (1990).
[21] Z. Zhang and S. Satpathy, Phys. Rev. Lett. **65**, 2650 (1990).
[22] M. Plihal and A. A. Maradudin, Phys. Rev. B **44**, 8565 (1991).